OXFORD

Human Molecular Genetics, 2015, Vol. 24, No. 9 2662–2672

doi: 10.1093/hmg/ddv030
Advance Access Publication Date: 29 January 2015
Original Article

ORIGINAL ARTICLE

Rett syndrome like phenotypes in the R255X *Mecp2* mutant mouse are rescued by *MECP2* transgene

Meagan R. Pitcher[1,4], José A. Herrera[1,4], Shelly A. Buffington[2], Mikhail Y. Kochukov[4], Jonathan K. Merritt[1,4,†], Amanda R. Fisher[5], N. Carolyn Schanen[6], Mauro Costa-Mattioli[2] and Jeffrey L. Neul[1,3,4,*,†]

[1]Interdepartmental Program in Translational Biology and Molecular Medicine, [2]Department of Neuroscience, Memory and Brain Research Center and [3]Department of Pediatrics, Section of Neurology, Baylor College of Medicine, Houston, TX, USA, [4]Jan and Dan Duncan Neurological Research Institute, Texas Children's Hospital, Houston, TX, USA, [5]Department of Biological Sciences, University of Delaware, Newark, DE, USA and [6]Nemours/Al DuPont Hospital for Children, Wilmington, DE, USA

*To whom correspondence should be addressed. Email: jneul@bcm.edu, jneul@ucsd.edu

Abstract

Rett syndrome (RTT) is a severe neurodevelopmental disorder that is usually caused by mutations in *Methyl-CpG-binding Protein 2* (*MECP2*). Four of the eight common disease causing mutations in *MECP2* are nonsense mutations and are responsible for over 35% of all cases of RTT. A strategy to overcome disease-causing nonsense mutations is treatment with nonsense mutation suppressing drugs that allow expression of full-length proteins from mutated genes with premature in-frame stop codons. To determine if this strategy is useful in RTT, we characterized a new mouse model containing a knock-in nonsense mutation (p.R255X) in the *Mecp2* locus (*Mecp2*^{R255X}). To determine whether the truncated gene product acts as a dominant negative allele and if RTT-like phenotypes could be rescued by expression of wild-type protein, we genetically introduced an extra copy of *MECP2* via an *MECP2* transgene. The addition of *MECP2* transgene to *Mecp2*^{R255X} mice abolished the phenotypic abnormalities and resulted in near complete rescue. Expression of *MECP2* transgene *Mecp2*^{R255X} allele also rescued mTORC1 signaling abnormalities discovered in mice with loss of function and overexpression of *Mecp2*. Finally, we treated *Mecp2*^{R255X} embryonic fibroblasts with the nonsense mutation suppressing drug gentamicin and we were able to induce expression of full-length MeCP2 from the mutant p.R255X allele. These data provide proof of concept that the p.R255X mutation of *MECP2* is amenable to the nonsense suppression therapeutic strategy and provide guidelines for the extent of rescue that can be expected by re-expressing MeCP2 protein.

Introduction

Rett syndrome (RTT) is a neurodevelopmental disorder that affects 1 in 10 000 live female births (1). Affected individuals have apparently normal initial neurocognitive development but then present with head growth deceleration and loss of acquired language and motor function. This devastating disease currently has no cure and people with RTT require lifelong care. The vast majority (>95%) of people with RTT have mutations in the X-chromosome transcriptional regulator *Methyl CpG binding Protein 2* (*MECP2*) (2), whose protein product, MeCP2, plays an important role in neuronal development by binding methylated CpG (3) and regulating expression of neuronal genes (4–6). A number of mouse models of RTT have been generated, with the most commonly used ones representing a complete loss of function of the

† Present address: M/C 0626, Department of Neurosciences, 9500 Gilman Drive, University of California, San Diego, La Jolla, CA 92093-0626, USA.
Received: December 17, 2014. **Revised:** January 19, 2015. **Accepted:** January 26, 2015

protein due to the elimination of the bulk of the coding sequence. Male mice with these large *MECP2* deletions show severe phenotypes early in life culminating in premature death, while female, heterozygous, mice develop symptoms of variable severity (7,8). Previously, it has been demonstrated that restoration of *Mecp2* expression in either pre-symptomatic (9) or post-symptomatic (10,11) mice can rescue abnormal phenotypes and premature death, providing hope that treatments can be developed to modify or even completely reverse the disease in humans.

Hundreds of different mutations in *MECP2* have been associated with RTT and the spectrum of RTT disease-causing mutations in *MECP2* include missense, nonsense, insertions and deletions; however, over 60% of RTT cases are caused by eight common point mutations in *MECP2* (p.R106W, p.R133C, p.T158M, p.R168X, p.R255X, p.R270X, p.R294X, p.R306C) (12). The eight common mutations arise due to C to T transitions at hypermutable CpG sites within the gene (13,14). Notably, four of the eight common disease causing mutations are nonsense mutations and are responsible for at least 35% of RTT cases (12,15), which presents an opportunity for mutation-specific therapy based on compounds that suppress nonsense mutations ('read through drugs'). Nonsense suppression was first identified as a property of aminoglycosides that act by binding with the ribosomal small subunit and increasing the incidence of mispairing of a near-cognate aminoacyl-tRNA (16). Aminoglycosides and non-aminoglycoside compounds have been used in animal disease models for cystic fibrosis (17) and Duchenne muscular dystrophy (18) to restore protein expression and correct deleterious phenotypes in mice with nonsense mutations; however to date, these therapies have not been used for a central nervous system disease such as RTT.

In order to test these compounds in RTT, an animal model with high construct and face validity expressing a human disease causing nonsense mutation in *MECP2* is necessary. Previously, a mouse expressing p.R168X was developed, but the engineering removed the carboxy-terminus of the gene, making it inappropriate for testing read through drugs (19). More recently, another p.R168X mouse was developed, but no formal characterization of the phenotype of the animal has been presented (20). In order to address these issues and develop a system to test the abilities of read through drugs to treat RTT, we generated a new mouse model of RTT containing a common nonsense mutation in *MECP2*, p.R255X (*Mecp2*^{R255X}). The utility of such a model is that it reproduces the clinical features observed in people with the disease. Furthermore, in anticipation of preclinical treatment trials, it is important to clearly define the severity of the phenotypes in order to adequately power experiments to look for improvement. To this end, we performed detailed phenotypic characterization of both male and female animals with *Mecp2*^{R255X}. Additionally, a theoretical concern with nonsense mutations is that there is the possibility that a truncated protein product produced may act as a dominant negative protein, interfering with any wild-type protein function. A dominant negative effect would severely limit the ability of a read through drug to show benefit, as it is unlikely that read through would 'correct' all the transcripts present. In the case of the p.R255 mutation, the mutation lies distal to the DNA-binding domain but disrupts the transcription repression domain of MeCP2. Therefore, it is possible that a protein containing only the DNA binding domain would be formed and potentially act as a dominant negative protein. To determine if the p.R255X allele has a dominant negative effect, we introduced the *MECP2* transgene (*Mecp2*$^{1Hzo/J}$) (21) to *Mecp2*^{R255X} to determine if providing a wild-type copy of MeCP2 was sufficient to rescue the phenotypes observed in this new RTT model. Finally, we used cells derived from *Mecp2*$^{R255X/Y}$ animals to demonstrate that an aminoglycoside, gentamicin, is able to read through and allow full-length protein production.

Results

Introduction of p.R255X mutation into *Mecp2* affects mRNA and protein expression

We generated a knock-in mouse carrying a p.R255X mutation (Fig. 1A) in the endogenous mouse *Mecp2* locus. From hemibrains of adult WT and *Mecp2*$^{R255X/Y}$ mice, we isolated mRNA and performed quantitative real-time PCR to detect the *Mecp2* exon 1; exon 3 splice junction and exon 3. *Mecp2*$^{R255X/Y}$ express both *Mecp2* mRNAs at ~60% level of WT (Fig. 1B). From contralateral hemibrains, we performed immunoblotting against the N-terminus of MeCP2 common to isoforms 1 and 2 but saw no evidence of protein product, even in the predicted size range of 20 kDa expected for a truncated protein produced from *Mecp2*$^{R255X/Y}$ (Supplementary Material, Fig. S1A) (19). We also performed immunoblotting against the common N-terminus from hippocampus and cortex lysates of adult WT and *Mecp2*$^{R255X/Y}$ mice and did not detect any MeCP2 full-length protein or truncation product in *Mecp2*$^{R255X/Y}$ (Fig. 1C). As expected, transgenic animals containing an extra copy of *Mecp2* (*Mecp2*$^{1Hzo/J}$) (21) express two times the amount of MeCP2 protein, and when this transgene is combined with *Mecp2*^{R255X} allele, a wild-type level of MeCP2 protein is observed (Fig. 1C).

As we were surprised to find no truncated protein product produced, we decided to see if this was also the case in people with RTT. We thus obtained human brain lysates from deceased RTT individuals and performed immunoblotting against the common MeCP2 amino-terminus. We did not detect any MeCP2 truncation product in heterozygous, female humans with the RTT-causing mutations p.R168X, p.R255X, p.R270X or K256 fsX288 (Fig. 1D). Because p.R255X mice do not express any MeCP2 protein or truncation product, we expected them to have phenotypic onset and severity similar to complete null MeCP2 mouse models (7,22).

Mecp2^{R255X} mice have abnormal brain, heart, breathing and weight phenotypes

As observed in humans with RTT (23) and other mouse models of RTT (8,24), *Mecp2*$^{R255X/Y}$ have decreased brain weight compared with WT (Fig. 2A). At age 6–8 weeks, *Mecp2*$^{R255X/Y}$ have increased breathing rate at baseline and when exposed to a hypoxic gas challenge (Fig. 2B). *Mecp2*$^{R255X/Y}$ over 8 weeks age had increased corrected QT interval time (Fig. 2C) and incidence of arrhythmia (Fig. 2D). All of these detrimental phenotypes were rescued by *MECP2*^{Tg1} allele (Fig. 2A–D). Notably, male *MECP2*^{Tg1} mice also had increased incidence of arrhythmia compared with wild-type littermates which was rescued in the presence of the p.R255X allele (Fig. 2D). *Mecp2*$^{R255X/+}$ female mice were assessed after 8 months age and had phenotypes similar to males (Fig. 2E–G) with abnormal phenotypes in brain weight, inappropriate response to hypoxic gas challenge and increased QT interval corrected by *MECP2*^{Tg1}. Three of six *Mecp2*$^{R255X/+}$ had arrhythmias, but this was not significant (Fig. 2H). Again, providing a wild-type copy of *Mecp2* corrected phenotypes in *Mecp2*$^{R255X/+}$ animals (Fig. 2E–H), similar to the rescue observed in male animals.

Mecp2$^{R255X/Y}$ were underweight at weaning (Supplementary Material, Fig. S2A), but recovered to WT body weight by 6 weeks age. *Mecp2*$^{R255X/Y}$ had liver and heart weights comparable with WT (Supplementary Material, Fig. S2B and C) at 8 weeks age.

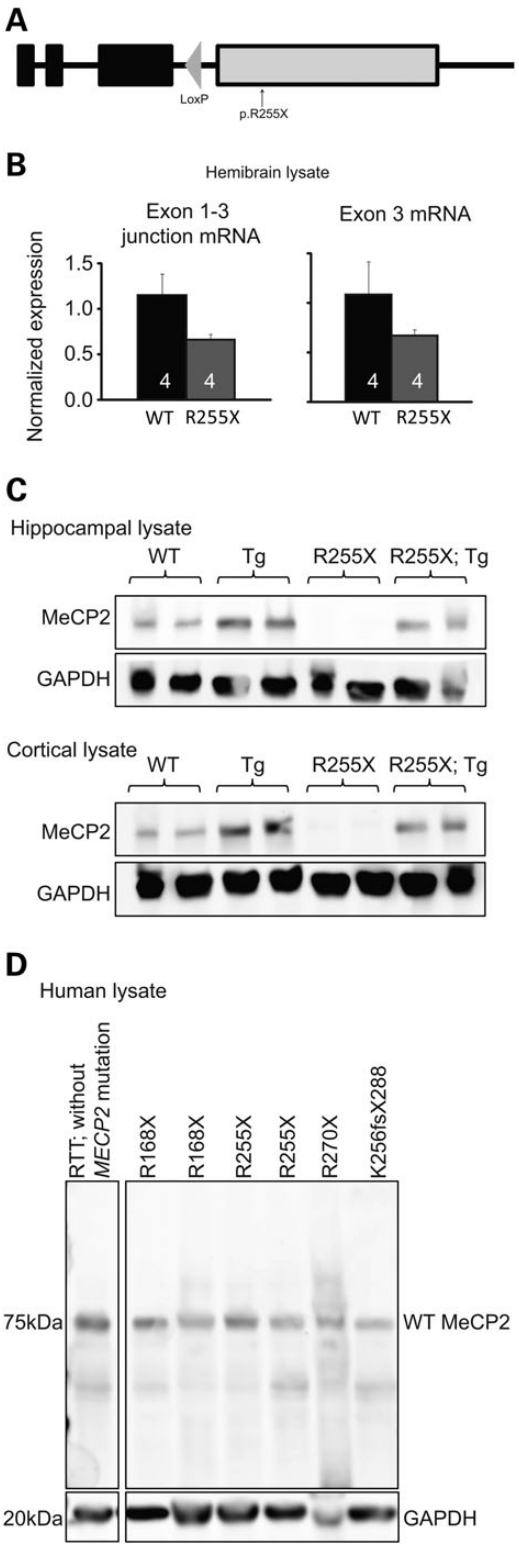

Figure 1. Introduction of R255X mutation into Mecp2 affects mRNA and protein expression. (**A**) Diagrammatic representation of the p.R255X allele. The allele has a single retained loxP sequence within intron 3, the expected nonsense point mutation in exon 4 and no other molecular changes in the locus, confirmed by sequencing. (**B**) Quantitative PCR of hemibrain lysates reveals that *Mecp2*$^{R255X/Y}$ mice brains express *Mecp2* mRNA at ~60% of WT levels. (**C**) Western blotting shows no full-length or truncated MeCP2 protein produced from the hippocampus or cortex of *Mecp2*$^{R255X/Y}$ mice brains. In contrast, brain tissue from Tg1 animals express twice as much MeCP2 as WT, and the addition of Tg1 transgene normalizes MeCP2 protein levels in *Mecp2*$^{R255X/Y}$ mice brains. (**D**) Western blot of human brain lysates from heterozygous female RTT patients who have nonsense mutations in *MECP2*. No truncation MeCP2 protein product was observed in any of the cases. Lower panel shows levels of GAPDH, which is used as a loading control.

Normal body weight was maintained in *Mecp2*$^{R255X/Y}$ until death, which occurred prematurely, with a median survival of 61 days, $\sigma = 1.764$ (Fig. 2I). *Mecp2*$^{R255X/+}$ developed an overweight body weight phenotype by 10 weeks age (Supplementary Material, Fig. S2D) and increased liver and heart weight by 8 months age (Supplementary Material, Fig. S2E and F). Abnormal body, liver and heart weight in *Mecp2*$^{R255X/+}$ was rescued by *MECP2*^{Tg1} allele. Body weight is a phenotype in *Mecp2* knockout mice which is dependent on genetic strain background (7). In a pure C57Bl6 background, *Mecp2* knockout mice have an underweight phenotype (7); however, an overweight body weight phenotype has been previously described in male *Mecp2* knockout mice in an isogenic 129S6/C57Bl6 background (25,26). In this study, the *Mecp2*^{R255X} experimental mice examined for body weight were from the N1–N5 generation of a backcross from the 129S6 to C57Bl6 strain background and the mixed genetic background could account for the weight dysregulation observed in male and female animals. Four *Mecp2*$^{R255X/+}$ had premature death (Fig. 2J), with two having tonic-clonic seizures followed by death after being handled. The remaining *Mecp2*$^{R255X/+}$ assessed for survival time lived to over 1 year age and the median survival in *Mecp2*$^{R255X/+}$ was 224 days, $\sigma = 31.768$. The premature death phenotype in *Mecp2*$^{R255X/Y}$ and *Mecp2*$^{R255X/+}$ was rescued by *MECP2*^{Tg1} (Fig. 2I and J).

Mecp2^{R255X} mice have anxiety, motor and learning impairments

At ~6 weeks age, several abnormal behavioral phenotypes were apparent in *Mecp2*$^{R255X/Y}$ mice. *Mecp2*$^{R255X/Y}$ mice made more entries into, traveled greater distance (Supplementary Material, Fig. S3A and B) and spent increased time in (Fig. 3A) the open arm of the elevated plus maze compared with WT mice. The decreased anxiety phenotype was rescued in the *Mecp2*$^{R255X/Y}$; *MECP2*^{Tg1} animals. *Mecp2*$^{R255X/Y}$ mice had motor coordination dysfunction demonstrated by increased footslips when walking on an array of parallel bars (Fig. 3B), decreased ability to remain suspended on a ¼ in diameter dowel (Fig. 3C), and impaired ability to learn the accelerating rotating rod walking task (Fig. 3D). *MECP2*^{Tg1} rescued all motor coordination phenotypes observed in *Mecp2*$^{R255X/Y}$ mice. In contextual fear conditioning—a hippocampal-dependent learning task (27)—*Mecp2*$^{R255X/Y}$ had impaired contextual long-term memory (Fig. 3E), which was rescued in the presence of *MECP2*^{Tg1}.

We tested female mice beginning at ~17 weeks age, an age at which abnormal behavioral phenotypes in female *Mecp2*$^{null/+}$ mouse models can be observed (28). There was no difference in behavior among the female genotypes in the elevated plus maze (Fig. 3G and Supplementary Material, Fig. S3C and D). *Mecp2*$^{R255X/+}$ had increased footslips in the parallel rod walking task (Fig. 3H) and difficulty learning the rotating rod walking task (Fig. 3J) compared with WT and MECP2^{Tg1} rescued both phenotypes. There was no difference among female mice in the motor coordination task of dowel hang time (Fig. 3I).

Mecp2$^{R255X/Y}$ have LTP impairment insurmountable by *MECP2*^{Tg1}

Mice expressing a truncated allele of *Mecp2* have impaired long-term potentiation (LTP) (29), while *MECP2*^{Tg1} mice have

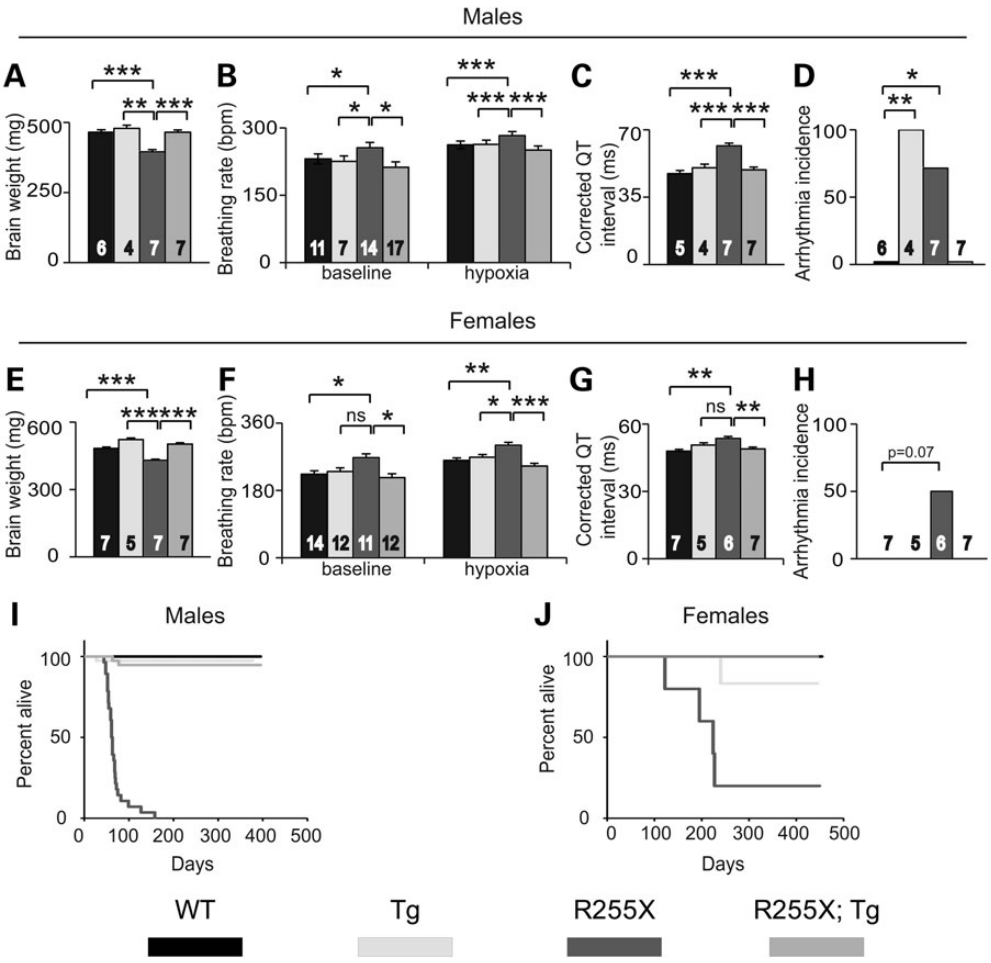

Figure 2. R255X mice have abnormal brain, heart, breathing and weight phenotypes. (**A**) *Mecp2*$^{R255X/Y}$ mice have decreased brain weight compared with WT and this phenotype is rescued by *MECP2*^{Tg1}. (**B**) *Mecp2*$^{R255X/Y}$ mice have increased breathing rate at baseline normal air conditions and when exposed to a hypoxic environment. (**C**) *Mecp2*$^{R255X/Y}$ have increased Q–T interval compared with WT and this phenotype is rescued by *MECP2*^{Tg1}. (**D**) *Mecp2*$^{R255X/Y}$ has increased occurrence of arrhythmia compared with WT and this phenotype is corrected by transgene. (**E**) *Mecp2*$^{R255X/+}$ mice have decreased brain weight compared with WT and this phenotype is rescued by *MECP2*^{Tg1}. (**F**) *Mecp2*$^{R255X/+}$ mice have increased breathing rate at baseline normal air conditions and when exposed to a hypoxic environment. (**G**) *Mecp2*$^{R255X/+}$ have increased Q—T interval compared with WT and this phenotype is rescued by *MECP2*^{Tg1}. (**H**) *Mecp2*$^{R255X/+}$ have increased incidence of arrhythmia. (**I**) Male and (**J**) female R255X mice have reduced survival compared with WT. The premature death phenotype is rescued by *MECP2*^{Tg1}. ***$P < 0.001$, **$P < 0.01$, *$P < 0.05$. Error bars are SEM. See Supplementary Material, Table S1 for full details regarding number of animals in each group at each age and full statistical comparisons.

enhanced LTP (21). To determine if expression of *MECP2*^{Tg1} on the *Mecp2*$^{R255X/Y}$ background could rescue hippocampal synaptic plasticity, we performed field recordings on acute hippocampal slices from 6- to 7-week-old male mice of each genotype. Despite rescue of contextual learning in the presence of the *MECP2*^{Tg1} allele, both *Mecp2*$^{R255X/Y}$ and *Mecp2*$^{R255X/Y}$; *MECP2*^{Tg1} had decreased evoked field excitatory post-synaptic potential (fEPSP) slope compared with WT and *MECP2*^{Tg1} (Fig. 4). Surprisingly, *MECP2*^{Tg1} did not display the previously described enhancement of LTP after high-frequency stimulation of Schaffer-collateral synapses (21). Despite the presence of protein in the hippocampus (Fig. 1C), the *MECP2*^{Tg1} is unable to rescue the LTP phenotype caused by lack of MeCP2 in the hippocampus of *Mecp2*$^{R255X/Y}$; *MECP2*^{Tg1} animals.

Mecp2$^{R255X/Y}$ and *Mecp2*^{Tg1} have mTORC1 pathway abnormalities

To determine the molecular mechanism underlying the behavioral and cellular phenoytpes in *MECP2*^{Tg1} and *Mecp2*$^{R255X/Y}$, we analyzed the activity of mammalian target of rapamycin complex 1 (mTORC1), a key signaling pathway underlying long-term changes in synaptic strength and behavioral learning (30–33). The best characterized mechanism by which mTORC1 controls LTP and memory is through its control of new protein synthesis (30). mTORC1 regulates mRNA translation rates through phosphorylation of its downstream effectors, eIF4E-binding proteins (4E-BPs) and p70 S6 kinase (S6K) (30). We determined mTORC1 activity by measuring the phosphorylation levels of the direct downstream target of S6K ribosomal protein S6 (S6) in region-specific brain lysates across genotypes. S6 is phosphorylated at S240/244 and S235/236. The S240/244 phosphorylation site on S6 is targeted by mTORC1-S6K, whereas S235/236 is phosphorylated by both S6K and mitogen-activated protein kinase (MAPK/ERK) (34). We did not observe any differences in MAPK/ERK activity among genotypes (Supplementary Material, Fig. S4A–D). Therefore, we measured whether mTORC1 activity is altered in *Mecp2*$^{R255X/Y}$ mice, *MECP2*^{Tg1} mice and double-mutant *Mecp2*$^{R255X/Y}$;*MECP2*^{Tg1} mice. Impaired mTORC1 signaling was previously reported in a cellular model of RTT, where exon 3 was ablated (35). Consistent with these results, in the

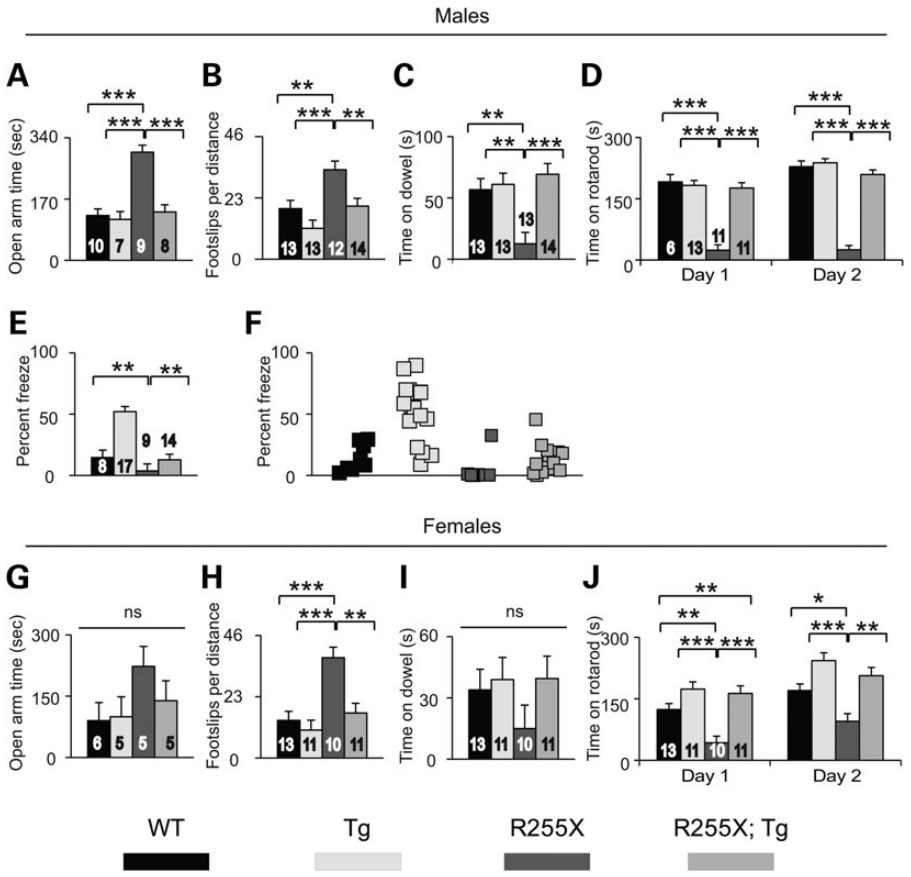

Figure 3. R255X mice have anxiety, motor and learning impairments. (**A**) *Mecp2*$^{R255X/Y}$ mice spend increased time in the open arms of the elevated plus maze compared with WT and this phenotype is rescued by *MECP2*^{Tg1}. (**B**) *Mecp2*$^{R255X/Y}$ mice have increased footslips in the parallel rod walking task compared with WT and this phenotype is rescued by *MECP2*^{Tg1}. (**C**) *Mecp2*$^{R255X/Y}$ mice have decreased hang time on ¼" diameter dowel compared with WT and this phenotype is rescued by *MECP2*^{Tg1}. (**D**) *Mecp2*$^{R255X/Y}$ mice perform poorly on the accelerating rotating rod walking task and do not show motor learning behavior, and this phenotype is rescued by *MECP2*^{Tg1}. (**E** and **F**) *Mecp2*$^{R255X/Y}$ mice have reduced context freeze response in the conditioned fear learning task compared with WT and this phenotype is rescued by *MECP2*^{Tg1}. (**G**) There is no difference in open arm time among the four female genotypes in the elevated plus maze. (**H**) *Mecp2*$^{R255X/+}$ mice have increased footslips in the parallel rod walking task compared with WT and this phenotype is rescued by *MECP2*^{Tg1}. (**I**) There is no difference in dowel hang time among the four female genotypes. (**J**) *Mecp2*$^{R255X/+}$ mice do not learn the accelerating rotating rod walking task and have reduced time on the rotarod compared with WT and this phenotype is rescued by *MECP2*^{Tg1}. ***$P < 0.001$, **$P < 0.01$, *$P < 0.05$. Error bars are SEM. See Supplementary Material, Table S2 for full details regarding number of animals in each group at each age and full statistical comparisons.

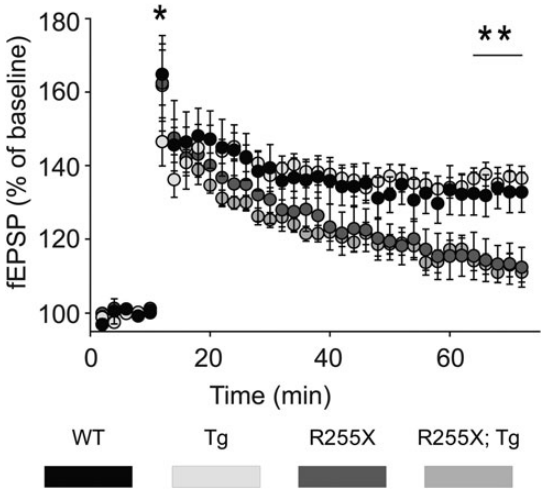

Figure 4. LTP phenotype is not rescued by *Tg*. *Mecp2*$^{R255X/Y}$ and *Mecp2*$^{R255X/Y}$; *MECP2*^{Tg1} have decreased fEPSP compared with WT in CA1 region of the hippocampus.

hippocampus and cerebellum of *Mecp2*$^{R255X/Y}$ mice, mTORC1 activity was reduced as determined by decreased phosphorylation of S6 at S235/236. Furthermore, S6 phosphorylation was reduced at both sites (S240/244 and S235/236) in the brainstem and cortex (Fig. 5A–D). Conversely, mTORC1 activity was near-uniformly increased across *MECP2*^{Tg1} brain regions (Fig. 5A–D).

Given that relative to WT, S240/244 S6 phosphorylation was mildly decreased in the cortex of *MECP2*^{Tg1}, but significantly increased relative to *Mecp2*$^{R255X/Y}$, and double-mutant mice (*MECP2*^{Tg1}, *Mecp2*$^{R255X/Y}$) show normal behaviors, we measured mTORC1 activity in these mice. Remarkably, mTORC1 signaling was restored in double-mutant mice across several brain regions (Fig. 5B–D). Taken together, our findings suggest that normalized mTORC1 signaling in the *Mecp2*^{R255X} brainstem, cerebellum and cortex by *MECP2*^{Tg1} expression could drive the restoration of motor, anxiety and premature death phenotypes in these mice.

An intriguing finding was that while in *Mecp2*$^{R255X/Y}$; *MECP2*^{Tg1} double mutants, contextual fear memory was rescued (Fig. 3E), hippocampal LTP was not (Fig. 4). S240/244 phosphorylation was rescued in *Mecp2*$^{R255X/Y}$; *MECP2*^{Tg1} hippocampal lysates,

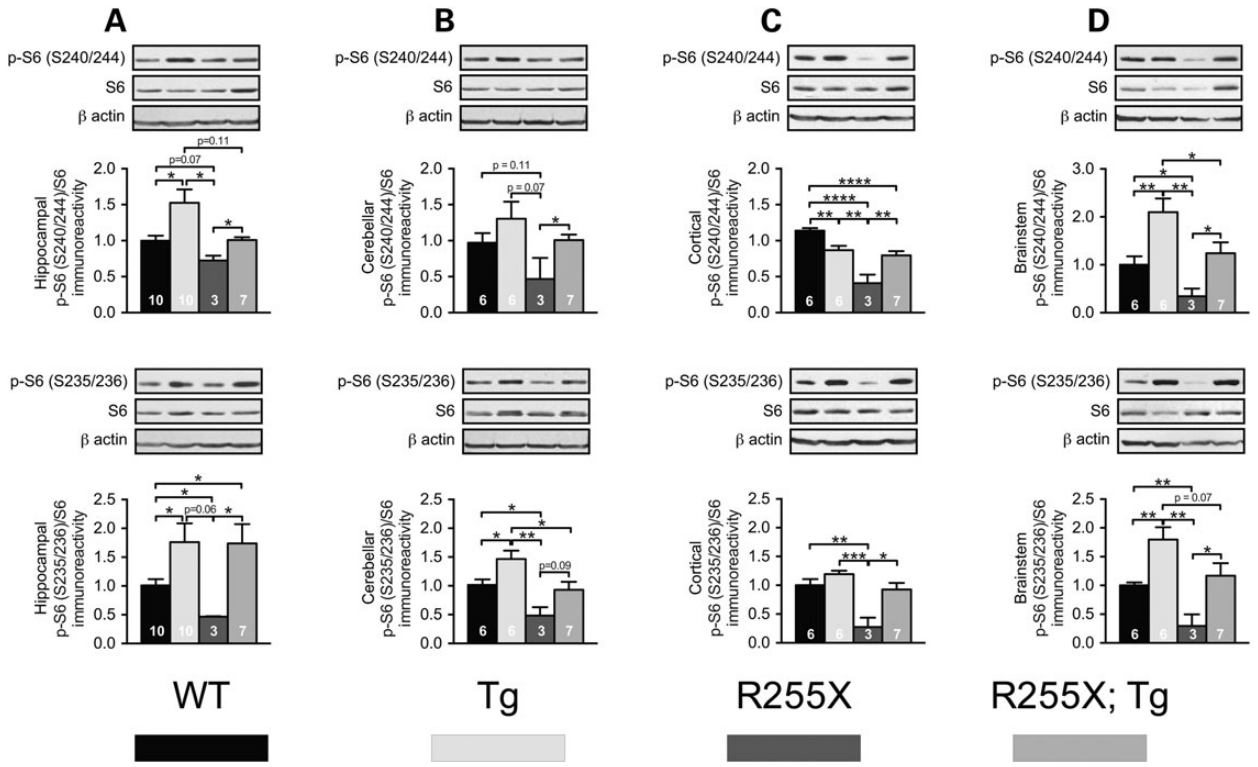

Figure 5. R255X and Tg have disrupted mTORC1 signaling. (**A**) Western blots from hippocampal lysates showing increased phosphorylation of S6 at S240/244 [$n = 10$ mice/genotype, $P = 0.0151$, $t(18) = 2.69$] and S235/236 [$P = 0.041$, $t(18) = 2.20$] in $MECP2^{Tg1}$ and decreased phosphorylation at S6 S240/244 [$n = 10$WT, 3$Mecp2^{R255X/Y}$, $P = 0.066$, $t(11) = 2.04$] and S6 S235/236 [$P = 0.023$, $t(11) = 2.65$] in $Mecp2^{R255X/Y}$. S6 phosphorylation at S240/244 is rescued by $MECP2^{Tg1}$ [$Mecp2^{R255X/Y}$: $Mecp2^{R255X/y}$; $MECP2^{Tg1}$ $P = 0.011$, $t(8) = 3.90$], but S235/236 phosphorylation remains elevated as in the $MECP2^{Tg1}$ [$Mecp2^{R255X/Y}$: $Mecp2^{R255X/Y}$; $MECP2^{Tg1}$ $P = 0.043$, $t(8) = 2.40$]. (**B**) Western blotting of cerebellar lysates shows trend toward reduced S6 S240/244 phosphorylation in $Mecp2^{R255X}$ mice [$P = 0.072$, $t(7) = 2.12$] with an opposite trend toward increased S240/244 phosphorylation in $MECP2^{Tg1}$ mice. Among the three mutant genotypes, $Mecp2^{R255X}$; $MECP2^{Tg1}$ cerebellar phospho-S6 S240/244 levels are most similar to WT, suggesting rescue by $MECP2^{Tg1}$ expression. A statistically significant decrease in phosphorylation of S6 S235/236 was noted in $Mecp2^{R255X/Y}$ mice [$P = 0.016$, $t(7) = 3.15$] and is rescued by $MECP2^{Tg1}$. In the cerebellum, $MECP2^{Tg1}$ mice have increased phosphorylation of S6 at S235/236 [$P = 0.030$, $t(11) = 2.50$]. (**C**) Similarly, western blotting from cortical lysates of $Mecp2^{R255X/Y}$ shows decreased phosphorylation of S6 at S235/236 [$P = 0.0065$, $t(7) = 3.83$] and S240/244 [$P < 0.0001$, $t(7) = 9.50$], with phosphorylation of both sites rescued by $MECP2^{Tg1}$. In the cortex, $MECP2^{Tg1}$ mice have decreased phosphorylation of S6 S240/244 [$P = 0.029$, $t(11) = 2.51$]. (**D**) Western blotting from brainstem lysates of $Mecp2^{R255X/Y}$ shows decreased phosphorylation of S6 at S235/236 and S240/244, with phosphorylation of both sites rescued by $MECP2^{Tg1}$ [$n = 3$ $Mecp2^{R255X/Y}$, 7 $Mecp2^{R255X}$;$MECP2^{Tg1}$; S240/244 $P = 0.042$, $t(8) = 2.42$; S235/236 $P = 0.046$, $t(8) = 2.37$]. $MECP2^{Tg1}$ mice have increased phosphorylation of S6 at S240/244 and S235/236 in the brainstem [S240/244 $P = 0.0097$, $t(11) = 3.12$; S235/236 $P = 0.0046$, $t(10) = 3.64$]. $MECP2^{Tg1}$ expression in the $Mecp2^{R255X/Y}$ background normalizes S6 phosphorylation at S240/244 and S235/236 to WT levels.

while S235/236 phosphorylation remained elevated as in $MECP2^{Tg1}$ (Fig. 5A). These results are consistent with the normalization of contextual fear memory we observed and suggest that hypoactive hippocampal mTORC1 signaling critically contributes to the contextual fear memory deficits in RTT mice; however, why the LTP phenotype of the $Mecp2^{R255X}$ mutation was not similarly rescued by $MECP2^{Tg1}$ expression remains unexplained by these data. In future studies, it will be important to identify other molecular alterations that could explain the impaired hippocampal LTP demonstrated in the $Mecp2^{R255X/Y}$; $MECP2^{Tg1}$ mice.

Rescue of wild-type MeCP2 expression in $Mecp2^{R255X/Y}$ mouse embryonic fibroblasts after treatment with gentamicin

The ultimate goal of the generation of this new knock-in nonsense allele of *Mecp2* is to test the ability of read through drugs to restore expression of MeCP2 protein. As a proof of concept, we utilized mouse embryonic fibroblasts (MEFs) generated from E13.5 $Mecp2^{R255X/Y}$ and WT littermate control embryos. As expected, $Mecp2^{R255X/Y}$-derived MEFs exposed to vehicle media do not express any MeCP2 protein (Fig. 6A). In contrast, exposure to 800 µg/ml gentamicin sulfate for 72 h incubation allowed expression of full-length MeCP2 from $Mecp2^{R255X/Y}$-derived MEFs (Fig. 6A) at a level of 75% of wild-type (Fig. 6B). Gentamicin exposure appears to increase the expression of the nuclear protein loading control histone H3 in treated WT fibroblasts; however, this effect is not significant. In a previous study, fibroblasts from patients with RTT were treated with gentamicin and there was a similar non-significant variable effect of gentamicin on the expression of the nuclear protein loading control emerin (36).

Discussion

Nonsense mutations are a common source of disease in a variety of conditions, and notably a major source of disease in RTT, with over 35% of all affected individuals having a nonsense mutation (12,15). The recent development of 'read through' compounds provides a novel, mutation-specific approach toward treatment of genetic diseases associated with nonsense mutations and the best progress has occurred in cystic fibrosis and Duchenne muscular dystrophy. In order to determine the efficacy of these drugs in central nervous system diseases such as RTT, it is necessary to have cellular and animal models containing clearly

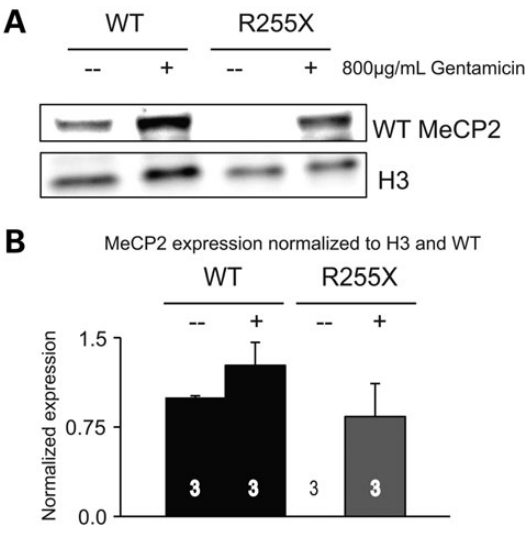

Figure 6. Read through compound treatment rescues MeCP2 expression *in vitro*. (**A**) Representative western blot demonstrating no full-length MeCP2 protein from MEFs derived from *Mecp2*$^{R255X/Y}$ mice after vehicle treatment, but full-length MeCP2 protein after 72 h treatment with 800 μg/ml gentamicin. Top panel was probed using an antibody against MeCP2, bottom panel probed with antibody against histone H3 (H3) as a loading control. (**B**) Quantitation of western blots as shown in (A) representing the three technical replicates examined per group.

defined nonsense mutations. To this end, here we generated and characterized a new mouse model of RTT. We clearly demonstrated that mice expressing this nonsense allele show the complete spectrum of phenotypes expected. As a proof of concept, we genetically introduced a wild-type copy of *Mecp2* and demonstrated that this effectively rescues the phenotypic spectrum observed in both male and female animals. This provides us with evidence that read through compounds could potentially treat this disease, and defines the optimal degree of success that might be expected, thus allowing us to correctly power future experiments with these drugs. This new model shows a high degree of face and construct validity and will be a useful tool in future drug development.

In addition to the detailed phenotypic characterization of the mouse model, we used the animals to generate a cellular model of the disease, which allows for efficient testing of the molecular ability of read through drugs to effectively allow the production of full-length protein. Here, we clearly demonstrated as a proof of concept that gentamicin can act in this manner to produce full-length protein from this allele. The renal toxicity of aminoglycosides such as gentamicin limit their use clinically; however, a variety of new aminoglycoside- and non-aminoglycoside based compounds have been developed that show markedly improved toxicity profiles. Future work will be directed at testing these newer compounds in the cellular model, and then bringing effective compounds *in vivo* to show therapeutic potential.

Surprisingly, *Mecp2* mRNA levels were decreased in tissue from *Mecp2*$^{R255X/Y}$ mice, and no truncated protein product observed. It is currently unclear why *Mecp2* mRNA levels are reduced in this allele. Previous work on a missense mutation in *Mecp2*, p.T158A, did not result in any changes in *Mecp2* mRNA, but the mutated protein showed decreased stability resulting in protein levels of ~60% of wild-type levels (37). In contrast, a previously generated nonsense mutation in *Mecp2*, p.R168X, showed reduced mRNA expression (~50% wild-type levels) and the production of a small (25 kDa) truncation product (19). One possible explanation for the reduced mRNA level observed in *Mecp2*$^{R255X/Y}$ mice is nonsense-mediated decay (NMD) (38); however, this specific nonsense mutation is contained in the final exon of the gene, a feature which usually prevents NMD. Another possibility is that MeCP2 regulates its own transcription, and in the situation in which no functional MeCP2 protein is produced, transcription also declines. Regardless of the exact mechanism, the fact that mRNA levels are decreased may be an important issue to address in order to maximize the potential therapy of read through compounds. It may be necessary to develop methods to increase transcription of *Mecp2* in order to increase available mRNA transcripts for the read through compounds to act upon. Interestingly, previous work has indicated that treatment with drugs such as fluoxetine can increased *Mecp2* mRNA. Discovering the molecular mechanisms involved in the transcriptional control of *Mecp2* may be a useful line of future experimentation.

The lack of observable protein product from the p.R255X mouse may have a variety of explanations. A real concern is that this lack of protein is some oddity that results from the genetic engineering used to create the allele. The lack of any observable truncated protein product from brain tissue isolated from people with truncating *MECP2* mutations argues against this. Biological alternatives include decreased stability of the truncated protein product, and other mechanisms such as mislocation of mutant *Mecp2* mRNA within stress granules, thus interfering with translation. Decreased protein stability is likely, given recent results showing decreased stability of MeCP2 containing a missense mutation (37); however this formally has not been proven here. The fact that gentamicin was able to cause full-length protein production from the p.R255X allele *in vitro* argues against mRNA mislocation and translation inhibition; however, exploring whether there is any mislocation of mutated *Mecp2* mRNA may be useful as it may point to another potentially targetable mechanism to improve read through treatments.

Addition of a single wild-type copy of *Mecp2* was highly efficient in rescuing the whole animal phenotypes observed; however, this genetic manipulation was not sufficient to restore normal LTP in hippocampal slice culture. Interestingly, we did not observe the expected increase in LTP previously reported in hippocampal slice culture from the *MECP2*^{Tg1} animals, although we did see the increased learning behavior reported in the conditioned fear assay (21). The results are internally consistent—rescue is achieved for the phenotype that displays the overexpression phenotype (conditioned fear overlearning) but not for the phenotype we fail to observe the overexpression phenotype (hippocampal LTP). Our inability to observe this slice culture phenotype may be explained by the differences in genetic strain background between the initial study (FVB) and this current work (C57Bl6). It is very interesting that the whole animal behavior phenotype is improved in the face of isolated circuit abnormalities, which speaks to the understanding that behavior phenotypes are not a function solely of a single isolated neural circuit but rather the ensemble of interrelated circuits.

Our exploration of mTORC1 signaling provides mechanistic insight into how *MECP2*^{Tg1} expression in the *Mecp2*^{R255X} background rescues several RTT mouse phenotypes. As previously reported (35), we found that loss of *Mecp2* leads to decreased mTORC1 signaling across brain regions. Intriguingly, we also determined that increased MeCP2 in the *MECP2*^{Tg1} animals leads to hyperactive mTORC1 signaling. mTORC1 activity is rescued in most *Mecp2*$^{R255X/Y}$; *Mecp2*^{Tg1} brain regions, with the notable exception of the hippocampus. Here, S235/236 phosphorylation remains elevated as in *MECP2*^{Tg1}. Importantly, despite the failure of the Tg to rescue the p.R255X-associated hippocampal LTP

deficits, restoration of hippocampal mTORC1 activity did correlate with normalized contextual learning. Thus, our findings suggest that restoration of mTORC1 signaling in both RTT models could be useful treatment strategies.

mTORC1 dysfunction has been implicated in a variety of neurodevelopmental disorders (39), most notably in tuberous sclerosis complex (TSC). TSC results from mutations in TSC1 or TSC2, which together function as negative upstream regulators of mTORC1 (40). Recent therapeutic approaches in TSC have focused on reducing mTORC1 activity through treatment with either rapamycin or its analogs, 'rapalogs' (39). Our observation of mTORC1 hyperactivity in mice overexpressing MeCP2 suggests that a similar treatment strategy might prove effective in treating people with Xq28 duplication syndrome. In contrast, deficient mTORC1 activity in RTT suggests a need to take an opposite therapeutic approach, namely stimulating mTORC1 activity. In future work, it could be interesting to test whether pharmacological inhibition of Pten (phosphatase and tensin homolog), an upstream negative regulator of mTORC1 activity (39), in the brain could rescue some of the pathophysiological phenotypes seen in the *Mecp2*$^{R255X/Y}$ RTT model.

Previous work has shown that neurotrophic growth factors such as *Brain derived neurotrophic factor* (*Bdnf*) (41) or *Insulin-like growth factor 1* (*Igf1*) (42,43) are able to partially reverse phenotypes in mice lacking MeCP2 function. Both of these growth factors increase mTORC1 activity via the PI3K/Akt pathway, which may account for at least some of the beneficial effects of these compounds in RTT. Ultimately, RTT and Xq28 duplication syndrome may be among the many neurodevelopmental disorders linked to dysregulated mTORC1 activity (30,39); however, the causal relationship between MeCP2 function and mTORC1 remains to be determined. Our results suggest the interesting possibility that either increasing or decreasing mTORC1 signaling could be a new mechanism-based therapeutic approach to treat RTT and Xq28 duplication syndrome, respectively. The *MeCP2*$^{R255X/Y}$ animal and cellular models of MeCP2 dysfunction (both loss and gain of function) reported herein could therefore prove highly valuable in dissecting common mechanisms linking multiple neurodevelopmental disorders and aid in therapeutic development.

Materials and Methods

Mice

All methods and animal care procedures were approved by the Baylor College of Medicine Animal Care and Use Committee and were housed in AAALAC-approved facilities at Baylor College of Medicine. *Mecp2*$^{R255X/+}$ founder mice in the 129S6 background were mated to C57Bl6 *MECP2*^{Tg1} males. F1 isogenic mice *Mecp2*$^{R255X/X}$; *MECP2*^{Tg1} were then crossed to wild-type C57Bl6 (Jackson Laboratories). Experimental mice were from generations N1–N5 of a backcross from F1 *Mecp2*$^{R255X/X}$; *MECP2*^{Tg1} founders to C57Bl6 males.

Sequencing, quantitative PCR and immunoblotting of *Mecp2*

DNA fragments from WT and *Mecp2*$^{R255X/Y}$ mice were PCR amplified and cloned into TOPO-TA vector (Life Technologies). Sequencing was performed by Lone Star Sequencing (Houston, TX, USA) and assembled in DNASTAR. Three to four mice per genotype were humanely euthanized and brains quickly extracted and split into hemispheres. From one hemisphere, total RNA was extracted using Trizol (Invitrogen). First-strand cDNA was generated using SuperScript III (Invitrogen) and *Mecp2* was probed using SYBR Green methodology with previously described primers (44). From the contralateral hemibrain, frozen tissues were lysed in ice-cold homogenizing buffer [2% sodium dodecyl sulfate, 0.1 M Tris and protease inhibitor cocktail (Sigma), pH 7.5] with a Dounce homogenizer. Protein concentration was calculated by the colorimetric bicinchoninic acid method (Thermo Scientific). Thirty microgram protein were loaded to 4–12% gradient SDS–PAGE gel (Bio-rad) and run at 95 V for 1 h at 4°C. Gels were transferred to nitrocellulose membrane at 37 mA constant for 4 h at 4°C, blocked several hours in 5% bovine serum albumin in PBS plus 5% Tween, and then incubated overnight with antibodies to MeCP2 15–30 (Sigma) and GAPDH (Millipore). Membranes were incubated for 1 h with secondary antibodies conjugated to a Cy5 fluorophore (Jackson ImmunoResearch) and blots were imaged using the Cy5 channel in a GE Imager. Human lysate protein concentrations were unknown and the maximum loading volume was loaded and immunoblotted as above.

Western blotting of mTORC1 pathway

Behaviorally naïve, non-moribund, 7- to 9-week-old male mice were deeply anesthetized and their brains were rapidly dissected on ice. Brain regions, as specified, were isolated and tissue was flash frozen. Frozen tissue was lysed in ice-cold homogenizing buffer [200 mM HEPES, 50 mM NaCl, 10% Glycerol, 1% Triton X-100, 1 mM EDTA, 50 mM NaF, 2 mM Na_3VO_4, 25 mM β-glycerophosphate and EDTA-free complete ULTRA tablets (Roche, Indianapolis, IN, USA)]. Lysate protein concentration was assayed by the Bradford method (ThermoScientific, 23238) and lysates were resolved by 12.5% acrylamide SDS–PAGE. Gel contents were transferred overnight at 30 V to nitrocellulose membranes. Membranes were blocked 1 h at RT with 5% milk, 2% TWEEN-20 tris-buffered saline then incubated in primary antibody overnight. Secondary antibodies were applied for 1 h at RT and the blots were visualized using enhanced chemiluminescent substrates (ThermoScientific, 34095).

Primary antibodies used for western blotting include rabbit anti-phospho-S6 (S240/244) [Cell Signaling Technology (CST), #2215, 1:1000], rabbit anti-phospho-S6 (S235/236) (CST, #2211, 1:1000), mouse anti-S6 (CST, #2317,1:1000), rabbit anti-phospho-p42/44-MAPK/ERK (CST, #4370; 1:1000), rabbit anti-p42/44-MAPK/ERK (CST, #4695, 1:1000) and mouse anti-α-actin (Millipore, #1501, 1:1000). HRP-conjugated goat-anti-rabbit (Jackson ImmunoResearch, 111-035-144, 1:10 000) and goat-anti-mouse (Jackson ImmunoResearch, 115-035-003, 1:2000) secondary antibodies were used to visualize the primary antibody bands.

Characterization of mice

Weight, temperature, whole-body plethysmography and heart rate were recorded as described previously (45). Parallel rod walking (25), dowel walking and accelerating rotating rod were performed as described previously (44). Elevated plus maze was performed as described previously (46). The above-described data were analyzed using a one-way analysis of variance (ANOVA), followed by Tukey's *t*-test *post hoc* pairwise comparisons between all genotypes. Conditioned fear was performed as described previously (31) and analyzed by the Kruskal–Wallis non-parametric test followed by Mann–Whitney *U post hoc* test. Transthoracic electrocardiography and programmed electrical stimulation were performed as described previously (47) with

corrected QT data analyzed by one-way ANOVA, followed by Tukey's *t*-test and arrhythmias analyzed by χ^2. Survival statistics were calculated by the Kaplan–Meier, followed Tarone–Ware *post hoc*.

Hippocampal electrophysiology

In coronal slice, CA1 stimulation was performed with platinum/iridium parallel bipolar electrode 1 MΩ, 75 µm tip separation (Microprobes, Gaithersburg, MD, USA) on Schaffer-collaterals. The recording electrode was a glass pipette filled with artificial cerebrospinal fluid (2 MΩ). Evoked field excitatory post-synaptic potentials (fEPSP) were acquired using a Multiclamp 700b amplifier and a 1440a Digidata interface (Molecular Devices, Sunnyvale, CA, USA). Baseline stimulation rate was every 30 s at 35–65 µA (half-max fEPSP). LTP induction was performed using two 1 s 100 Hz pulse trains, separated by 30 s. Recording time was from 20 min before and 90 min after LTP induction. Data were analyzed using two-way ANOVA, followed by the Holm–Sidak *post hoc* test.

Tissue culture

MEFs from wild-type and mutant embryos were derived as described previously (48). Briefly, embryos were removed from the uterine horns of female mice on post-coital day 13.5 followed by dissection of embryo body from placenta, embryonic sac and head. Embryo bodies were minced in 0.05% trypsin–EDTA (Invitrogen) with DNAse 1 (GE Healthcare), incubated at 37°C for 15 min and centrifuged to form a cell pellet. The single-cell suspension was then plated in standard fibroblast media: Dulbecco's Modified Eagle Medium + l-glutamine (Life Technologies), 10% fetal bovine serum (Gemini) and 1× MEM Non-Essential Amino Acids Solution (Life Technologies). Fibroblasts lines were grown to passage 3 and genotyped for p.R255X allele. For drug studies, 5×10^5 fibroblasts were plated in 10 cm dishes and incubated in standard fibroblast media. Twenty-four hours after plating cells were treated with 800 µg/ml gentamicin sulfate (Sigma G1914) dissolved in standard fibroblast media or non-treated for 72 h. Treatment or non-treatment media was refreshed every 24 h. Cell lysates were prepared by trypsinizing the 10 cm dishes and lysing cellular membranes in 0.5% NP40, pH7.9 followed by centrifugation. Nuclear proteins were isolated from DNA and debris in the pellet using a 1 h high salt incubation (300 mM NaCl) on ice. Nuclear proteins were immunoblotted as described above using an in-house polyclonal antibody to MeCP2 N-308 and commercially available H3 antibody (Abcam ab1791).

Supplementary Material

Supplementary Material is available at *HMG* online.

Acknowledgements

We thank Dr Huda Zoghbi, Alana McCall and Mona Shahbazian for providing human brain extracts. We thank Diana Parra for technical assistance. We thank the Baylor College of Medicine Intellectual and Developmental Disorders Research Center (BCM IDDRC) Neurobehavioral Core (Director Richard Paylor and Corinne Spencer) for use of the facility.

Conflict of Interest statement. None declared.

Funding

This work was supported by US National Institutes of Health Grants R01HD062553 (J.L.N.), U54HD083092 and P30HD024064 (BCM IDDRC), NIH R01 NIMH 096816 and NIH NINDS 076708 (M.C.M) the International Rett Syndrome Foundation Grant #2906, the Anthony and Cynthia Petrello Scholar Fund, and in part by a grant to Baylor College of Medicine from the Howard Hughes Medical Institutes through the Med into Grad Initiative. The content is solely the responsibility of the authors and does not necessarily represent the official views of the National Institutes of Health or the *Eunice Kennedy Shriver* Child Health and Human Development Institute (NICHD).

References

1. Laurvick, C.L., de Klerk, N., Bower, C., Christodoulou, J., Ravine, D., Ellaway, C., Williamson, S. and Leonard, H. (2006) Rett syndrome in Australia: a review of the epidemiology. *J. Pediatr.*, **148**, 347–352.
2. Amir, R.E., Van den Veyver, I.B., Wan, M., Tran, C.Q., Francke, U. and Zoghbi, H.Y. (1999) Rett syndrome is caused by mutations in X-linked MECP2, encoding methyl-CpG-binding protein 2. *Nat. Genet.*, **23**, 185–188.
3. Nan, X., Meehan, R.R. and Bird, A. (1993) Dissection of the methyl-CpG binding domain from the chromosomal protein MeCP2. *Nucleic Acids Res.*, **21**, 4886–4892.
4. Chahrour, M., Jung, S.Y., Shaw, C., Zhou, X., Wong, S.T., Qin, J. and Zoghbi, H.Y. (2008) MeCP2, a key contributor to neurological disease, activates and represses transcription. *Science*, **320**, 1224–1229.
5. Nan, X., Ng, H.H., Johnson, C.A., Laherty, C.D., Turner, B.M., Eisenman, R.N. and Bird, A. (1998) Transcriptional repression by the methyl-CpG-binding protein MeCP2 involves a histone deacetylase complex. *Nature*, **393**, 386–389.
6. Jones, P.L., Veenstra, G.J., Wade, P.A., Vermaak, D., Kass, S.U., Landsberger, N., Strouboulis, J. and Wolffe, A.P. (1998) Methylated DNA and MeCP2 recruit histone deacetylase to repress transcription. *Nat. Genet.*, **19**, 187–191.
7. Guy, J., Hendrich, B., Holmes, M., Martin, J.E. and Bird, A. (2001) A mouse Mecp2-null mutation causes neurological symptoms that mimic Rett syndrome. *Nat. Genet.*, **27**, 322–326.
8. Chen, R.Z., Akbarian, S., Tudor, M. and Jaenisch, R. (2001) Deficiency of methyl-CpG binding protein-2 in CNS neurons results in a Rett-like phenotype in mice. *Nat. Genet.*, **27**, 327–331.
9. Luikenhuis, S., Giacometti, E., Beard, C.F. and Jaenisch, R. (2004) Expression of MeCP2 in postmitotic neurons rescues Rett syndrome in mice. *Proc. Natl Acad. Sci. USA*, **101**, 6033–6038.
10. Giacometti, E., Luikenhuis, S., Beard, C. and Jaenisch, R. (2007) Partial rescue of MeCP2 deficiency by postnatal activation of MeCP2. *Proc. Natl Acad. Sci. USA*, **104**, 1931–1936.
11. Guy, J., Gan, J., Selfridge, J., Cobb, S. and Bird, A. (2007) Reversal of neurological defects in a mouse model of Rett syndrome. *Science*, **315**, 1143–1147.
12. Neul, J.L., Fang, P., Barrish, J., Lane, J., Caeg, E.B., Smith, E.O., Zoghbi, H., Percy, A. and Glaze, D.G. (2008) Specific mutations in methyl-CpG-binding protein 2 confer different severity in Rett syndrome. *Neurology*, **70**, 1313–1321.
13. Wan, M., Lee, S.S., Zhang, X., Houwink-Manville, I., Song, H.R., Amir, R.E., Budden, S., Naidu, S., Pereira, J.L., Lo, I.F. *et al.* (1999) Rett syndrome and beyond: recurrent spontaneous and familial MECP2 mutations at CpG hotspots. *Am. J. Hum. Genet.*, **65**, 1520–1529.

14. Rideout, W.M. 3rd, Coetzee, G.A., Olumi, A.F. and Jones, P.A. (1990) 5-Methylcytosine as an endogenous mutagen in the human LDL receptor and p53 genes. *Science*, **249**, 1288–1290.
15. Cuddapah, V.A., Pillai, R.B., Shekar, K.V., Lane, J.B., Motil, K.J., Skinner, S.A., Tarquinio, D.C., Glaze, D.G., McGwin, G., Kaufmann, W.E. *et al.* (2014) Methyl-CpG-binding protein 2 (MECP2) mutation type is associated with disease severity in Rett syndrome. *J. Med. Genet.*, **51**, 152–158.
16. Keeling, K.M., Wang, D., Conard, S.E. and Bedwell, D.M. (2012) Suppression of premature termination codons as a therapeutic approach. *Crit. Rev. Biochem. Mol. Biol.*, **47**, 444–463.
17. Du, M., Jones, J.R., Lanier, J., Keeling, K.M., Lindsey, J.R., Tousson, A., Bebok, Z., Whitsett, J.A., Dey, C.R., Colledge, W.H. *et al.* (2002) Aminoglycoside suppression of a premature stop mutation in a Cftr−/− mouse carrying a human CFTR-G542X transgene. *J. Mol. Med. (Berl.)*, **80**, 595–604.
18. Barton-Davis, E.R., Cordier, L., Shoturma, D.I., Leland, S.E. and Sweeney, H.L. (1999) Aminoglycoside antibiotics restore dystrophin function to skeletal muscles of mdx mice. *J. Clin. Invest.*, **104**, 375–381.
19. Lawson-Yuen, A., Liu, D., Han, L., Jiang, Z.I., Tsai, G.E., Basu, A. C., Picker, J., Feng, J. and Coyle, J.T. (2007) Ube3a mRNA and protein expression are not decreased in Mecp2R168X mutant mice. *Brain Res.*, **1180**, 1–6.
20. Brendel, C., Belakhov, V., Werner, H., Wegener, E., Gartner, J., Nudelman, I., Baasov, T. and Huppke, P. (2011) Readthrough of nonsense mutations in Rett syndrome: evaluation of novel aminoglycosides and generation of a new mouse model. *J. Mol. Med. (Berl.)*, **89**, 389–398.
21. Collins, A.L., Levenson, J.M., Vilaythong, A.P., Richman, R., Armstrong, D.L., Noebels, J.L., David Sweatt, J. and Zoghbi, H.Y. (2004) Mild overexpression of MeCP2 causes a progressive neurological disorder in mice. *Hum. Mol. Genet.*, **13**, 2679–2689.
22. Stearns, N.A., Schaevitz, L.R., Bowling, H., Nag, N., Berger, U.V. and Berger-Sweeney, J. (2007) Behavioral and anatomical abnormalities in Mecp2 mutant mice: a model for Rett syndrome. *Neuroscience*, **146**, 907–921.
23. Jellinger, K. and Seitelberger, F. (1986) Neuropathology of Rett syndrome. *Am. J. Med. Genet. Suppl.*, **1**, 259–288.
24. Belichenko, N.P., Belichenko, P.V., Li, H.H., Mobley, W.C. and Francke, U. (2008) Comparative study of brain morphology in Mecp2 mutant mouse models of Rett syndrome. *J. Comp. Neurol.*, **508**, 184–195.
25. Pitcher, M.R., Ward, C.S., Arvide, E.M., Chapleau, C.A., Pozzo-Miller, L., Hoeflich, A., Sivaramakrishnan, M., Saenger, S., Metzger, F. and Neul, J.L. (2013) Insulinotropic treatments exacerbate metabolic syndrome in mice lacking MeCP2 function. *Hum. Mol. Genet.*, **22**, 2626–2633.
26. Ward, C.S., Arvide, E.M., Huang, T.W., Yoo, J., Noebels, J.L. and Neul, J.L. (2011) MeCP2 is critical within HoxB1-derived tissues of mice for normal lifespan. *J. Neurosci.*, **31**, 10359–10370.
27. Kim, J.J. and Fanselow, M.S. (1992) Modality-specific retrograde amnesia of fear. *Science*, **256**, 675–677.
28. Samaco, R.C., McGraw, C.M., Ward, C.S., Sun, Y., Neul, J.L. and Zoghbi, H.Y. (2012) Female Mecp2(+/−) mice display robust behavioral deficits on two different genetic backgrounds providing a framework for pre-clinical studies. *Hum. Mol. Genet.*, **22**, 96–109.
29. Moretti, P., Levenson, J.M., Battaglia, F., Atkinson, R., Teague, R., Antalffy, B., Armstrong, D., Arancio, O., Sweatt, J.D. and Zoghbi, H.Y. (2006) Learning and memory and synaptic plasticity are impaired in a mouse model of Rett syndrome. *J. Neurosci.*, **26**, 319–327.
30. Buffington, S.A., Huang, W. and Costa-Mattioli, M. (2014) Translational control in synaptic plasticity and cognitive dysfunction. *Annu. Rev. Neurosci.*, **37**, 17–38.
31. Stoica, L., Zhu, P.J., Huang, W., Zhou, H., Kozma, S.C. and Costa-Mattioli, M. (2011) Selective pharmacogenetic inhibition of mammalian target of Rapamycin complex I (mTORC1) blocks long-term synaptic plasticity and memory storage. *Proc. Natl Acad. Sci. USA*, **108**, 3791–3796.
32. Helmstetter, F.J., Parsons, R.G. and Gafford, G.M. (2008) Macromolecular synthesis, distributed synaptic plasticity, and fear conditioning. *Neurobiol. Learn. Mem.*, **89**, 324–337.
33. Gafford, G.M., Parsons, R.G. and Helmstetter, F.J. (2013) Memory accuracy predicts hippocampal mTOR pathway activation following retrieval of contextual fear memory. *Hippocampus*, **23**, 842–847.
34. Ruvinsky, I. and Meyuhas, O. (2006) Ribosomal protein S6 phosphorylation: from protein synthesis to cell size. *Trends Biochem. Sci.*, **31**, 342–348.
35. Li, Y., Wang, H., Muffat, J., Cheng, A.W., Orlando, D.A., Loven, J., Kwok, S.M., Feldman, D.A., Bateup, H.S., Gao, Q. *et al.* (2013) Global transcriptional and translational repression in human-embryonic-stem-cell-derived Rett syndrome neurons. *Cell Stem Cell*, **13**, 446–458.
36. Vecsler, M., Ben Zeev, B., Nudelman, I., Anikster, Y., Simon, A. J., Amariglio, N., Rechavi, G., Baasov, T. and Gak, E. (2011) Ex vivo treatment with a novel synthetic aminoglycoside NB54 in primary fibroblasts from Rett syndrome patients suppresses MECP2 nonsense mutations. *PLoS One*, **6**, e20733.
37. Goffin, D., Allen, M., Zhang, L., Amorim, M., Wang, I.T., Reyes, A.R., Mercado-Berton, A., Ong, C., Cohen, S., Hu, L. *et al.* (2011) Rett syndrome mutation MeCP2 T158A disrupts DNA binding, protein stability and ERP responses. *Nat. Neurosci.*, **15**, 274–283.
38. Giannandrea, M., Guarnieri, F.C., Gehring, N.H., Monzani, E., Benfenati, F., Kulozik, A.E. and Valtorta, F. (2013) Nonsense-mediated mRNA decay and loss-of-function of the protein underlie the X-linked epilepsy associated with the W356x mutation in synapsin I. *PLoS One*, **8**, e67724.
39. Costa-Mattioli, M. and Monteggia, L.M. (2013) mTOR complexes in neurodevelopmental and neuropsychiatric disorders. *Nat. Neurosci.*, **16**, 1537–1543.
40. Inoki, K., Li, Y., Zhu, T., Wu, J. and Guan, K.L. (2002) TSC2 is phosphorylated and inhibited by Akt and suppresses mTOR signalling. *Nat. Cell Biol.*, **4**, 648–657.
41. Chang, Q., Khare, G., Dani, V., Nelson, S. and Jaenisch, R. (2006) The disease progression of Mecp2 mutant mice is affected by the level of BDNF expression. *Neuron*, **49**, 341–348.
42. Tropea, D., Giacometti, E., Wilson, N.R., Beard, C., McCurry, C., Fu, D.D., Flannery, R., Jaenisch, R. and Sur, M. (2009) Partial reversal of Rett Syndrome-like symptoms in MeCP2 mutant mice. *Proc. Natl Acad. Sci. USA*, **106**, 2029–2034.
43. Castro, J., Garcia, R.I., Kwok, S., Banerjee, A., Petravicz, J., Woodson, J., Mellios, N., Tropea, D. and Sur, M. (2014) Functional recovery with recombinant human IGF1 treatment in a mouse model of Rett Syndrome. *Proc. Natl Acad. Sci. USA*, **111**, 9941–9946.
44. Samaco, R.C., Fryer, J.D., Ren, J., Fyffe, S., Chao, H.T., Sun, Y., Greer, J.J., Zoghbi, H.Y. and Neul, J.L. (2008) A partial loss of function allele of methyl-CpG-binding protein 2 predicts a human neurodevelopmental syndrome. *Hum. Mol. Genet.*, **17**, 1718–1727.
45. Ward, C.S., Arvide, E.M., Huang, T.W., Yoo, J., Noebels, J.L. and Neul, J.L. (2011) MeCP2 is critical within HoxB1-derived

tissues of mice for normal lifespan. *J. Neurosci.*, **31**, 10359–10370.
46. Lugo, J.N., Swann, J.W. and Anderson, A.E. (2014) Early-life seizures result in deficits in social behavior and learning. *Exp. Neurol.*, **256**, 74–80.
47. McCauley, M.D., Wang, T., Mike, E., Herrera, J., Beavers, D.L., Huang, T.W., Ward, C.S., Skinner, S., Percy, A.K., Glaze, D.G. *et al.* (2011) Pathogenesis of lethal cardiac arrhythmias in Mecp2 mutant mice: implication for therapy in Rett syndrome. *Sci. Transl. Med.*, **3**, 113ra125.
48. Jozefczuk, J., Drews, K. and Adjaye, J. (2012) Preparation of mouse embryonic fibroblast cells suitable for culturing human embryonic and induced pluripotent stem cells. *J. Vis. Exp.*, **64**, 3854.